Published in final edited form as:
J Biomech. 2014 February 7; 47(3): 659–666. doi:10.1016/j.jbiomech.2013.11.048.

Interaction of Lubricin with Collagen II Surfaces: Adsorption, Friction, and Normal Forces

Debby P. Chang[1,2], **Farshid Guilak**[1,3,4], **Gregory Jay**[5], and **Stefan Zauscher**[1,2,3,*]

[1] Department of Mechanical Engineering and Materials Science, Duke University, Durham NC 27708

[2] Center for Biologically Inspired Materials and Material Systems, Duke University, Durham NC 27708

[3] Center for Biomolecular and Tissue Engineering, Duke University, Durham NC 27708

[4] Department of Orthopaedic Surgery, Duke University, Durham NC 27710

[5] Department of Emergency Medicine, Rhode Island Hospital, Providence, RI 02903

Abstract

One of the major constituents of the synovial fluid that is thought to be responsible for chondroprotection and boundary lubrication is the glycoprotein lubricin (PRG4); however, the molecular mechanisms by which lubricin carries out its critical functions still remain largely unknown. We hypothesized that the interaction of lubricin with type II collagen, the main component of the cartilage extracellular matrix, results in enhanced tribological and wear properties. In this study, we examined: i) the molecular details by which lubricin interacts with type II collagen and how binding is related to boundary lubrication and adhesive interactions; and, ii) whether collagen structure can affect lubricin adsorption and its chondroprotective properties. We found that lubricin adsorbs strongly onto denatured, amorphous, and fibrillar collagen surfaces. Furthermore, we found large repulsive interactions between the collagen surfaces in presence of lubricin, which increased with increasing lubricin concentration. Lubricin attenuated the large friction and also the long-range adhesion between fibrillar collagen surfaces. Interestingly, lubricin adsorbed onto and mediated the frictional response between the denatured and native amorphous collagen surfaces equally and showed no preference on the supramolecular architecture of collagen. However, the coefficient of friction was lowest on fibrillar collagen in the presence of lubricin. We speculate that an important role of lubricin in mediating interactions at the cartilage surface is to attach to the cartilage surface and provide a protective coating that maintains the contacting surfaces in a sterically repulsive state.

*Corresponding Author Professor Stefan Zauscher Department of Mechanical Engineering and Materials Science 144 Hudson Hall P.O. Box 90300 Durham, NC 27708 zauscher@duke.edu Phone: (919) 660-5360 Fax: (919) 660-5409.

Conflict of Interest
The authors have no conflict of interest to declare.

Keywords

Colloidal Probe Microscopy; Lateral Force Microscopy; Atomic Force Microscope; Friction; Tribology; PRG4; Wear; Glycoproteins; Collagen; Type II Collagen Lubricin; SAMs; Boundary Lubrication

Introduction

In healthy joints, articular cartilage provides an extremely efficient load-bearing surface and exhibits extraordinary lubrication and wear (Ateshian, 2009; Katta et al., 2008; Mow et al., 1992; Swanson, 1979). The superficial zone of articular cartilage and its thin, amorphous outermost layer, the lamina splendens, comprise the bearing surface for joint contact. This superficial zone consists of a mostly tangentially arranged collagen fibrillar network (Jeffery et al., 1991), and the adhesion of molecules to the cartilage surface is believed to contribute to its boundary lubrication properties (Chan et al., 2011a). Damage to this superficial zone, or absence of lubricating factors, may cause a cascade of mechanical and biological events that can lead to irreversible wear and joint disease such as osteoarthritis (Neu et al., 2010, Saarakkala, 2010 #33).

Lubricin, also called superficial zone protein (SZP) or proteoglycan-4 (PRG4), is found in the synovial fluid and also on the superficial zone of the articular cartilage, and is believed to contribute to the lubrication, wear resistance, and anti-adhesive properties of cartilage (Elsaid et al., 2005; Jay et al., 2001; Rhee et al., 2005; Schumacher et al., 1994; Swann et al., 1981). Lubricin is composed of 1404 amino acids, with a somatomedin-B (SMB)-like domain and a hemopexin (PEX)-like domain at its N- and C-terminal ends, respectively (Rhee et al., 2005). The hydrophilic center domain of lubricin is heavily glycosylated and partially capped with negatively charged sialic acid. Recent experiments confirmed that to function as an effective boundary lubricant, lubricin must adhere to the surface (Chang et al., 2009; Chang et al., 2008; Zappone et al., 2007). However, the details of lubricin binding to cartilage surfaces are still largely unknown (Nugent-Derfus et al., 2007).

Recent immunolocalization studies suggest that lubricin binds to the articular cartilage surface with its C-terminal end (Jones et al., 2007), which contains a hemopexin-like domain. This domain is conserved on many matrix metalloproteinases (MMPs), such as collagenases, where it mediates binding to native, triple helical collagen (Murphy and Knauper, 1997; Perumal et al., 2008; Tam et al., 2002), but not on denatured collagen (Tam et al., 2002). This finding suggests that besides unspecific interaction with the cartilage surface, binding to collagen is potentially important for anchoring lubricin to the cartilage surface. Type II collagen is the predominant type of collagen in articular cartilage, where it self-assembles into large, fibrillar aggregates and adopts a complex degree of structural organization (Mow et al., 1992; Sokoloff, 1978). A Monomeric type II collagen consists of three polypeptide strands, intertwined into a triple helical structure. Each triple-helix associates with its neighbors and forms microfibrils that are staggered regularly apart at a distance of 67 nm (Lehninger et al., 2000).

We hypothesized that lubricin has specific binding affinity to collagen II where it binds preferentially to triple helical collagen and mediates adhesion and friction. To test this hypothesis we used colloidal probe microscopy (CPM) to examine the conformational and tribological properties of lubricin on collagen surfaces to further understand the interaction and function of lubricin as a boundary lubricant and chondroprotectant in diarthrodial joints. Specifically, we used denatured collagen (without triple-helix structure), amorphous collagen (native triple helical collagen), and fibrillar collagen (aggregates of native triple

helical collagen), to determine the effect of collagen structure and conformation on lubricin binding. We also examined how lubricin interacts with collagen and what effect this binding has on friction and adhesion properties. Our results provide new insights into the molecular interactions of lubricin with collagen.

Materials and Methods

Materials

Lubricin was purified from human synovial fluid (Jay et al., 2001), and a series of lubricin solutions (50 - 400 μg/ml) was prepared from stock solution by dilution with phosphate buffered saline (Gibco, 1x PBS, 1mM KH_2PO_4, 155 mM NaCl, 3 mM Na_2HPO_4, pH 7.4). The concentration range was chosen to bracket the physiological value of ~200 μg/ml found in synovial fluid (Elsaid et al., 2005).

Type II collagen (from chicken sternal cartilage, Sigma Aldrich) was received as powder and dissolved in 0.25% acetic acid at 1mg/ml overnight at 4°C. For amorphous collagen, the dissolved collagen was diluted with PBS to 100 μg/ml concentration. For denatured collagen, the collagen solution was heated to 60°C for 15 minutes and then diluted with PBS. For fibrillar collagen, the dissolved collagen was allowed to self-assemble at physiological pH at room temperature until collagen strands were detectable with AFM.

Preparation of colloidal probes and substrate surfaces

Gold-coated colloidal probes, functionalized with alkanethiol self-assembled monolayers (SAMs) and various forms of collagen, were fabricated by gluing 10 μm diameter glass microspheres (Duke Scientific, Palo Alto, CA) to the end of AFM cantilevers (V-shaped Si_3N_4 cantilever with 0.58 N/m typical spring constant, Bruker-Veeco™) with a one part photo-curing epoxy (Norland Optical Adhesive #81) (Chang et al., 2008). The probes were then coated with a 5 nm chromium adhesion layer followed by a 45 nm gold layer using an e-beam evaporator (CHA Industries, Fremont, CA).

Type II collagen was chemically attached to gold-coated glass substrates and colloidal probes with glutaraldehyde coupling chemistry (Figure 1). First, the gold substrates and colloidal probes were cleaned with UV ozone for ~5 min, rinsed with 0.05% SDS, dH2O, and ethanol, and then incubated in 1mM NH_2-terminated SAM (cystamine hydrochloride, Sigma Aldrich) in ethanol overnight at room temperature. After incubation, the substrates were sonicated briefly to remove excess thiol (with exception of the colloidal probes) and then rinsed with copious amounts of ethanol and dried with nitrogen. The amine-terminated SAM were activated in 12% glutaric dialdehyde (Sigma Aldrich) for 30 minutes and then incubated in 100 μg/ml of the collagen solution of interest for over 2 hours. Fibrillar collagen substrates were obtained by chemically attaching the fibrils onto the substrate surface, using the procedure described above.

Characterization of Collagen Structure

CD—Circular dichroism spectroscopy (CD) was used to monitor the secondary molecular structure of collagen. The collagen solution with a concentration of 0.04 mg/ml in 0.25% acetic acid was measured with a CD spectrophotometer, equipped with a stirred thermoelectric cell holder (Aviv model 202 CD spectrophotometer). CD spectra were acquired over the wavelength range of 190-260 nm at 25°C before and after heating. The thermal denaturation of collagen was monitored by observing the CD signal at 220 nm over the range of 25-60 °C with a 10 s averaging time and a 2 min equilibration time. The resulting data were baseline corrected by solvent subtraction.

XPS—X-ray photoelectron spectroscopy (XPS) (Axis Ultra, Kratos Analytical) was used to verify the surface chemical composition. A monochromatic Al source was used (10 mA, 15 kV) for both the survey and high resolution scans. Survey spectra from 0 to 1200 eV were taken followed by high resolution scans around the C_{1s}, and N_{1s} regions. To avoid degradation of the nonconductive samples, charge neutralization with low energy electrons and a magnetic immersion lens was used. The spectra were shifted by setting the binding energy maximum of C_{1s} at 284.5 eV.

AFM—The substrate surfaces were imaged in Tapping Mode® with a Multimode AFM using a Nanoscope IIIa controller (Bruker-Veeco, Santa Barbara, CA) using an ultrasharp silicon tip (NSC14, MikroMasch, San Jose, CA). Fibrillar collagen formation was verified by AFM imaging, by incubating a freshly cleaved mica surface with ~40 μL collagen fibril solution for ~15min, followed by rinsing gently with MilliQ water, and drying under a stream of nitrogen. After chemical attachment, the collagen surfaces were imaged again at the lowest applied load.

Ellipsometry—Dry collagen film thicknesses were measured on a spectroscopic ellipsometer (M-88 Model 450, J. A. Woollam Co., Lincoln, NE) at 65°, 70°, and 75°. For each substrate, ellipsometric data was collected on the gold surface before and after collagen deposition. The collagen film thickness was obtained by fitting the ellipsometric data with a Cauchy dispersion model on top of the bare gold layer (Ma et al., 2004). The film thickness of each sample was measured at three different locations and is reported as an average value.

Contact Angle—A contact angle goniometer (Model 100, Rame-Hart Instrument Co., NJ) was used to measure the contact angle on the collagen substrates. Static contact angles were taken in ambient condition at room temperature with Milli-Q grade water (18.2 MΩcm) on at least 4 different locations on the same sample and reported as an average value.

Adsorption Measurements

Lubricin adsorption onto collagen surfaces was measured using surface plasmon resonance (SPR Biacore X instrument, Uppsala, Sweden) (Chang et al., 2008). Prior to any measurement, the substrate surfaces were first equilibrated with PBS (pH ~7.4), injected at a flow rate of 5 μL/min at 25°C. The adsorption of lubricin on collagen surfaces was achieved by sequential injection of 15 μl solution from 25 to 400 μg/ml concentrations. After each lubricin injection, a continuous flow of PBS was used to rinse away any loosely adsorbed molecules. The change in the response unit (RU) before and after each injection is proportional to the number of molecules adsorbed on surface. As a reference, for globular proteins, 1 ΔRU is equivalent to a surface coverage of approximately 1 pg/mm^2.

Force Measurement

A MFP-3D AFM (Asylum Research, Santa Barbara, CA) was used to measure the friction and normal interaction forces. The cantilever normal spring constant (k_n, nN/nm) was determined prior to any measurements from the power spectral density of the thermal noise fluctuations in air (Hutter and Bechhoefer, 1993) by fitting the first resonance peak to equations for a simple harmonic oscillator (Walters et al., 1996). The normal photodiode sensitivity (S, nm/V), was determined from the constant compliance regime upon approach against a hard substrate. The lateral calibration factor, (α, nN/V), was obtained by the wedge calibration method (Ogletree et al., 1996; Varenberg et al., 2003) with a 30° sloped Si calibration wedge (Tocha et al., 2006) using equations adapted for colloidal probes (Han et al., 2007).

Friction measurements were made as described previously (Chang et al., 2009). Briefly, friction was measured as a function of normal load by incrementally increasing the applied load from 0 nN to ~115 nN then incrementally decreasing the load until the tip separated from the surface. All friction measurements were performed over a scan area of 20×20μm and at a scan speed of 40 μm/s. Normal and lateral signals were monitored simultaneously over 256 scan lines, with the measured force values averaged over 256 points per scan line. The friction force was determined by taking half the difference between the lateral deflection signal obtained from the forward (trace) and backward (retrace) scans. Friction versus load data were obtained on the same region over the entire load range at three different locations. To assess any wear effect on friction force due to scanning, three repeated scan cycles on the same location were conducted. Lateral force measurements were performed in the presence of purified human lubricin (50, 100, 200, 400 μg/ml), after allowing 15 minutes of equilibration time between each change in concentration with the colloidal probe far removed from the substrate surface.

Results

Collagen Substrate Characterization

All collagen-coated substrates were prepared by chemically attaching collagen from a solution of interest to the substrate surface with glutaraldehyde. The topographical AFM images of the denatured, amorphous and fibrillar collagen surfaces showed distinct morphologies (Figure 2). For amorphous collagen coatings, a solution of native collagen was used, where the triple helical (coiled coil) structure is conserved. The presence of the coiled coil motif was verified by CD, where the spectrum showed a peak with a maximum at 220 nm (inset of Figure 3). For denatured collagen coatings, the collagen solution was subjected to a heat treatment. Collagen denaturation was verified by the absence of the peak maximum at 200 nm in the CD spectrum (Figure 3). For the fibrillar collagen coating, dissolved collagen was allowed to self-assemble into micro fibrils at physiological pH at room temperature, prior to chemical grafting to the substrate surface. Figure 2c shows that the triple helical collagen self-assembled into fibrils by aligning in parallel, staggered fashion, producing the characteristic cross-striation with a pitch of 66 nm (Meisenberg and Simmons, 1998) (inset of Figure 2c).

Ellipsometric measurements showed that the denatured and amorphous substrates have a dry film thickness of 3.2 ± 0.4 nm and 4.0 ± 0.1 nm, respectively. The fibrillar substrate, however, was too rough to yield accurate ellipsometric height values. Instead, AFM topographical images revealed collagen microfibril heights ranging from 35 to 150 nm. The root-mean-square (RMS) surface roughness over 20 by 20 μm scan areas of denatured, amorphous, and fibrillar collagen substrates were 4.6 nm, 3.4 nm, and 68.4 nm, respectively.

XPS survey spectra (Figure 4) and high resolution scans of the C_{1s} and N_{1s} regions (data not shown) were used to verify the presence of collagen on the substrate surfaces. The appearance of the N peak, from the nitrogen in the collagen, confirmed the successful immobilization of collagen. The N/C molar concentration ratio of the denatured, amorphous, and fibrillar collagen surfaces were around 0.26-0.32, which is in good agreement with the expected value of 0.32 from pure collagen and better than the 0.12 ratio obtained from a spin-coated collagen layer (Dupont-Gillain and Rouxhet, 2001). The contact angles of the denatured, amorphous, and fibrillar collagen substrates were 45°, 29°, and 34° ± 4°, respectively.

Adsorption Measurement

The adsorption of lubricin on denatured (heat-treated), amorphous (native), and fibrillar (native & self-assembled) collagen surfaces were measured by SPR (Figure 5). Lubricin adsorbed readily onto all three types of collagen surfaces, and the adsorbed amount increased gradually with increasing lubricin concentration. The adsorbed amount is similar on the denatured and amorphous collagen surfaces, and about 50% higher on the fibrillar collagen surface.

Normal Forces on Approach

Averaged AFM normal force curves were measured upon approach between a flat surface and a colloidal probe, both functionalized with collagen of interest (Figure 6). The normal forces between surfaces measured in presence of lubricin were repulsive and increased with increasing lubricin concentration. The extent of repulsion was similar for the three different types of collagen surfaces.

Adhesion Forces on Retraction

Adhesive interactions arose upon surface separation between collagen surfaces both in PBS and also in the presence of lubricin. Retraction force curves showed significant molecular stretching events (Figures 7a, b). In presence of lubricin, the stretching signature was similar to that previously observed between hydrophobic and hydrophilic surfaces (Chang et al., 2008) In absence of lubricin, molecular stretching of collagen molecules was observed. Between two fibrillar collagen surfaces, in absence of lubricin, these adhesive interactions persist over long retraction distance (Figure 7a). The distance at max pull-off force was approximately 1500 nm and was reduced with addition of lubricin (Figure 7c). In presence of lubricin, the maximum pull-off force was approximately 300 nm for all three types of collagen surfaces.

The adhesion energy, calculated from the area under the retraction curves, was relatively constant among the denatured, amorphous, and fibrillar collagen surfaces (Figure 7d). In presence of greater than 100 μg/ml of lubricin, the adhesion energy remained approximately constant, with an average adhesion energy of about 1 fJ (Figure 7d).

Friction Interaction

Friction forces were determined as a function of normal load between denatured, amorphous, and fibrillar collagen surfaces (Figures 8a-c), and the average coefficients of friction (COF), calculated from the slopes of the friction force vs. load curves, varied as a function of lubricin concentration (Figure 8d). Friction was high only on fibrillar collagen surfaces and in absence of lubricin; however, addition of as little as 50 μg/ml lubricin lowered the friction force substantially (Figure 8c). Interestingly, the frictional behavior in the presence of lubricin was largely independent of lubricin solution concentration and about the same for denatured and amorphous collagen surfaces (COF ≈ 0.2). On the other hand, the COF between fibrillar collagen surfaces in presence of lubricin was slightly lower at approximately 0.1.

Discussion

Although the presence of lubricin on articular cartilage surfaces has been shown to be essential in the boundary lubrication mechanism necessary for joint lubrication and joint health (Coles et al., 2010b; Elsaid et al., 2005; Jay et al., 2001; Rhee et al., 2005; Schmidt et al., 2007) details of the interaction between lubricin and the cartilage surface are still largely

unknown. Recent immunolocalization studies with recombinant lubricin revealed a specific binding affinity between the cartilage surface and the C-terminal ends of lubricin (Jones et al., 2007) suggesting a possible interaction between lubricin's hemopexin-like domain and the cartilage surface. This hemopexin-like domain is conserved on many matrix metalloproteinases (Murphy and Knauper, 1997) and has been shown to be involved in the binding, and possibly the unwinding, of native triple-helical collagen (Perumal et al., 2008). Interestingly, the hemopexin-like domain does not bind on denatured collagen (Tam et al., 2002).

In the current study, we investigated the interaction between lubricin and type II collagen, a major component of articular cartilage, in denatured, amorphous and fibrillar forms, and examined lubricin's ability to adhere and lubricate these collagen surfaces. Our findings showed that human lubricin adsorbed to all three types of collagen surfaces, where it effectively mediates the friction upon adsorption. The collagen II surfaces used in the present work are meant to serve as controlled model systems and thus do not include all the features of the native articular surface; however, this approach provides a controlled model system to investigate the specific interaction between lubricin and type II collagen. Collagen is present at or near the cartilage surface in multiple forms, and AFM images of cartilage surfaces reveal a wide range of surface structures, most of which are amorphous, acellular and largely non-fibrous (Coles et al., 2008; Jurvelin et al., 1996). Fibrillar collagen is seen on the superficial zone of the articular cartilage surface, where it is oriented tangentially to the surface and mostly formed by aggregation of collagen types II (80%), IX (10%), and XI (10%) (Bruckner and Vanderrest, 1994). Recent computational and molecular visualization studies showed that fibril architecture and triple-helical conformation govern collagen proteolysis (Perumal et al., 2008). It was shown that normal thermal fluctuations are sufficient to cause partial unwinding of the triple helix which allows collagenases to dock and lock onto collagen via their hemopexin domains. Here we hypothesized that akin to the collagenases, lubricin binds to triple helical collagen via lubricin's hemopexin-like domains.

The amounts of lubricin adsorbed on the three types of collagen surfaces (denatured, amorphous, or fibrillar) were approximately the same with a somewhat higher adsorption onto the fibrillar collagen substrate. We attribute this adsorption difference to the larger surface area presented by the fibrils compared with that by the planar coatings. The surface roughness of the fibrillar collagen substrate (RMS roughness = 68 nm) was more than an order of magnitude larger than that of the denatured and amorphous substrates (RMS roughness = 3-4 nm), which supports the notion that the available surface area for lubricin adsorption on the fibrillar substrate is much larger. The adsorbed amount of PRG4 on the model collagen surfaces is approximately 1-2 mg/m^2. This amount is less than the 7 mg/m^2 reported to be bound to superficial articular cartilage surfaces (Nugent-Derfus et al., 2007). Cartilage surfaces are, however, much rougher than our model surfaces, and thus the true area for adsorption is larger for cartilage surfaces, which likely explains the observed discrepancy of the amount of adsorbed PRG4. Our adsorption measurements show that lubricin adsorbs readily onto the three different types of collagen surfaces. This result is surprising, and suggests that lubricin binding does not depend on the availability of the triple helix structure or higher order collagen assembly, and possibly implies that the C-terminal hemopexin domain of lubricin is not critical for collagen binding. Clearly, further experiments are needed to ascertain the role of the C-terminal hemopexin-like domains for binding, such as experiments with deactivated hemopexin-like domains or truncated, engineered lubricin constructs. The current results support our previous findings (Chang et al., 2008) that lubricin is a highly surface-active molecule that can adsorb onto a wide variety of surfaces, including hydrophobic CH_3-terminated SAMs, hydrophilic OH-terminated SAMs, denatured collagen, amorphous collagen, fibrillar collagen, and even protein resistant tri-ethylene glycol-terminated SAMs.

The extent of repulsion between denatured and amorphous collagen surfaces was slightly larger than between the fibrillar surfaces. This observation can be explained by considering that the amorphous and denatured collagen coatings are highly hydrated, with collagen molecules extending into solution. These hydrated coatings are more easily compressed compared to the more tightly bound fibril bundles, which are less hydrated and much stiffer, and thus also significantly less compressible. In the presence of lubricin, large repulsive forces arise when two collagen surfaces are brought into close contact. The extent and strength of the long range, steric-entropic repulsion forces increase with increasing lubricin concentration. We found that the extent of the repulsive force is relatively similar between the denatured, amorphous and fibrillar collagen surfaces. In summary, the ability of lubricin to adhere to surfaces and exert repulsion forces is consistent with our previous studies on chemically uniform hydrophobic and hydrophilic surfaces (Chang et al., 2008) which further points to the potential role of lubricin as a chondroprotectant (Coles et al., 2010a).

Although interactions on approach were repulsive, adhesions between collagen surfaces occurred and were mediated by lubricin. The jagged adhesion force profiles observed here are characteristic of the stretching and breaking of molecular bridges that form between molecules tethering the surfaces. In absence of lubricin, the interactions between fibrillar collagen surfaces upon separation showed molecular stretching events to distances of approximately 1500 nm. This long-range force disappears after addition of lubricin, suggesting that lubricin shields the interaction between the collagen fibrils after adsorbing to the surface. The interaction distances upon separating two lubricin-coated collagen surfaces are similar to those observed on chemically uniform SAM surfaces (Chang et al., 2008). This finding further demonstrates lubricin's ability to prevent direct molecular interaction between the underlying substrates. An adhesive interaction between lubricin molecules upon surface separation was observed previously on hydrophobic and hydrophilic model surfaces (Chang et al., 2008). The finding that a lubricating agent can develop adhesion, while somewhat counterintuitive, is not entirely unreasonable. For example, recent nanomechanical studies showed self-adhesion between largely negatively charged cartilage glycosaminoglycans (GAGs) (Han et al., 2008) where this self-adhesion was proposed to play an important role in the structural and mechanical integrity of the cartilage tissue. Here, similar to GAGs, lubricin showed molecular chain entanglement or self-adhesion upon compression. This self-adhesion may have an important chondroprotective function, where the molecular chain interaction may enhance the shear resistance of the lubricin layer, thus maintaining the integrity of the cartilage surface under load (Coles et al., 2010a; Coles et al., 2010b).

Next we discuss the effect of lubricin on friction between denatured, amorphous, and fibrillar collagen surfaces (Figure 8). The COFs determined in the present study are quite similar to those measured in a cartilage-on-cartilage friction study (Schmidt et al., 2007). The COF on denatured and amorphous collagen surfaces was about 0.15 in PBS and increased slightly with addition of lubricin, i.e., there was no dose-dependent lubrication effect. These surfaces are smooth and hydrated, likely bearing a “brushy” collagen layer (see above), which contributes to boundary lubrication already in absence of lubricin. The slight increase in the COF with increasing amount of adsorbed lubricin is consistent with the additional forces the colloidal probe experiences while it is plowing through an increasingly viscous adsorbed layer. In contrast, the COF for fibrillar collagen surfaces sliding in PBS was much higher than that for the denatured and amorphous collagen surfaces, and was dramatically reduced upon addition of lubricin (Figures 8c,d). This friction behavior agrees with findings in the cartilage-on-cartilage friction study by Schmidt et al., who reported a COF of about 0.29 in PBS and a strong dose-dependent lubrication effect by PRG4 (Schmidt et al., 2007). In absence of lubricin, the rough, fibrillar collagen surfaces do not bear a sterically repulsive, hydrated layer, which likely explains the overall higher COF compared

with that for amorphous and denatured collagen surfaces. Taken together, our findings are consistent with previous studies that show that the boundary lubrication properties of cartilage are dependent on contact pressure as well as the presence of boundary lubricants at specific sites within the joint (Chan et al., 2011a, b).

In summary, we observed that lubricin binding to collagen II does not appear to depend on the molecular and supramolecular architecture of collagen, as similar binding behavior can be seen on denatured, amorphous and fibrillar collagen surfaces. Our findings further support the notion that lubricin is a highly surface active molecule which can adhere to a variety of surfaces. This calls in question whether lubricin's hemopexin-like domains are critically involved in binding to collagenous regions of the cartilage surface. Furthermore, we found that lubricin develops strong steric-repulsive interactions on all types of collagen surfaces to prevent direct surface contact, and thus mediates the adhesion and friction forces between the collagen surfaces. These findings support the hypothesis that lubricin plays an important role in maintaining the structural integrity of the cartilage surface and thus in promoting joint health by self-adhesion to provide a protective layer on the cartilage surface.

Acknowledgments

Supported by an NSF Early Career Award (SZ), NIH grants AR50245, AR48182, AR48852, and AG15768 (FG), and AR050180 (GDJ). We thank Jeffrey Coles for many useful discussions.

References

Ateshian GA. The role of interstitial fluid pressurization in articular cartilage lubrication. J Biomech. 2009; 42:1163–1176. [PubMed: 19464689]

Bruckner P, Vanderrest M. Structure and Function of Cartilage Collagens. Microscopy Research and Technique. 1994; 28:378–384. [PubMed: 7919525]

Chan SMT, Neu CP, Komvopoulos K, Reddi AH. Dependence of nanoscale friction and adhesion properties of articular cartilage on contact load. Journal of Biomechanics. 2011a; 44:1340–1345. [PubMed: 21316681]

Chan SMT, Neu CP, Komvopoulos K, Reddi AH. The role of lubricant entrapment at biological interfaces: Reduction of friction and adhesion in articular cartilage. Journal of Biomechanics. 2011b; 44:2015–2020. [PubMed: 21679953]

Chang DP, Abu-Lail NI, Coles JM, Guilak F, Jay GD, Zauscher S. Friction force microscopy of lubricin and hyaluronic acid between hydrophobic and hydrophilic surfaces. Soft Matter. 2009; 5:3438–3445. [PubMed: 20936046]

Chang DP, Abu-Lail NI, Guilak F, Jay GD, Zauscher S. Conformational mechanics, adsorption, and normal force interactions of lubricin and hyaluronic acid on model surfaces. Langmuir. 2008; 24:1183–1193. [PubMed: 18181652]

Coles JM, Blum JJ, Jay GD, Darling EM, Guilak F, Zauscher S. In situ friction measurement on murine cartilage by atomic force microscopy. Journal of Biomechanics. 2008; 41:541–548. [PubMed: 18054362]

Coles JM, Chang DP, Zauscher S. Molecular mechanisms of aqueous boundary lubrication by mucinous glycoproteins. Curr Opin Colloid In. 2010a; 15:406–416.

Coles JM, Zhang L, Blum JJ, Warman ML, Jay GD, Guilak F, Zauscher S. Loss of Cartilage Structure, Stiffness, and Frictional Properties in Mice Lacking PRG4. Arthritis and Rheumatism. 2010b; 62:1666–1674. [PubMed: 20191580]

Dupont-Gillain CC, Rouxhet PG. Modulable nanometer-scale surface architecture using spin-coating on an adsorbed collagen layer. Nano Letters. 2001; 1:245–251.

Elsaid KA, Jay GD, Warman ML, Rhee DK, Chichester CO. Association of articular cartilage degradation and loss of boundary-lubricating ability of synovial fluid following injury and inflammatory arthritis. Arthritis and Rheumatism. 2005; 52:1746–1755. [PubMed: 15934070]

Han L, Dean D, Daher LA, Grodzinsky AJ, Ortiz C. Cartilage Aggrecan Can Undergo Self-Adhesion. Biophys J. 2008; 95:4862–4870. [PubMed: 18676640]

Han L, Dean D, Ortiz C, Grodzinsky AJ. Lateral nanomechanics of cartilage aggrecan macromolecules. Biophys J. 2007; 92:1384–1398. [PubMed: 17142289]

Hutter JL, Bechhoefer J. Calibration of atomic force microscope tips. Rev. Sci. Instrum. 1993; 64:1868–1873.

Jay GD, Harris DA, Cha CJ. Boundary lubrication by lubricin is mediated by O-linked beta(1-3)Gal-GalNAc oligosaccharides. Glycoconjugate Journal. 2001; 18:807–815. [PubMed: 12441670]

Jeffery AK, Blunn GW, Archer CW, Bentley G. Three-dimensional collagen architecture in bovine articular cartilage. The Journal of bone and joint surgery. British. 1991; 73:795–801.

Jones ARC, Gleghorn JP, Hughes CE, Fitz LJ, Zollner R, Wainwright SD, Caterson B, Morris EA, Bonassar LJ, Flannery CR. Binding and localization of recombinant lubricin to articular cartilage surfaces. J Orthop Res. 2007; 25:283–292. [PubMed: 17106881]

Jurvelin JS, Muller DJ, Wong M, Studer D, Engel A, Hunziker EB. Surface and subsurface morphology of bovine humeral articular cartilage as assessed by atomic force and transmission electron microscopy. Journal of Structural Biology. 1996; 117:45–54. [PubMed: 8776887]

Katta J, Jin Z, Ingham E, Fisher J. Biotribology of articular cartilage--a review of the recent advances. Medical engineering & physics. 2008; 30:1349–1363. [PubMed: 18993107]

Lehninger, AL.; Nelson, DL.; Cox, MM. Lehninger principles of biochemistry. 3rd ed.. Worth Publishers; New York: 2000.

Ma HW, Hyun JH, Stiller P, Chilkoti A. “Non-fouling” oligo(ethylene glycol)-functionalized polymer brushes synthesized by surface-initiated atom transfer radical polymerization. Advanced Materials. 2004; 16:338.

Meisenberg, G.; Simmons, WH. Principles of medical biochemistry. Mosby; St. Louis: 1998.

Mow VC, Ratcliffe A, Poole AR. Cartilage and Diarthrodial Joints as Paradigms for Hierarchical Materials and Structures. Biomaterials. 1992; 13:67–97. [PubMed: 1550898]

Murphy G, Knauper V. Relating matrix metalloproteinase structure to function: Why the “hemopexin” domain? Matrix Biology. 1997; 15:511–518. [PubMed: 9138283]

Neu CP, Reddi AH, Komvopoulos K, Schmid TM, Di Cesare PE. Increased friction coefficient and superficial zone protein expression in patients with advanced osteoarthritis. Arthritis & Rheumatism. 2010; 62:2680–2687. [PubMed: 20499384]

Nugent-Derfus GE, Chan AH, Schumacher BL, Sah RL. PRG4 exchange between the articular cartilage surface and synovial fluid. J Orthop Res. 2007; 25:1269–1276. [PubMed: 17546655]

Ogletree DF, Carpick RW, Salmeron M. Calibration of frictional forces in atomic force microscopy. Review of Scientific Instruments. 1996; 67:3298–3306.

Perumal S, Antipova O, Orgel JPRO. Collagen fibril architecture, domain organization, and triple-helical conformation govern its proteolysis. Proceedings of the National Academy of Sciences of the United States of America. 2008; 105:2824–2829. [PubMed: 18287018]

Rhee DK, Marcelino J, Baker MA, Gong YQ, Smits P, Lefebvre V, Jay GD, Stewart M, Wang HW, Warman ML, Carpten JD. The secreted glycoprotein lubricin protects cartilage surfaces and inhibits synovial cell overgrowth. Journal of Clinical Investigation. 2005; 115:622–631. [PubMed: 15719068]

Schmidt TA, Gastelum NS, Nguyen QT, Schumacher BL, Sah RL. Boundary lubrication of articular cartilage: role of synovial fluid constituents. Arthritis Rheum. 2007; 56:882–891. [PubMed: 17328061]

Schumacher BL, Block JA, Schmid TM, Aydelotte MB, Kuettner KE. A Novel Proteoglycan Synthesized and Secreted by Chondrocytes of the Superficial Zone of Articular Cartilage. Archives of Biochemistry and Biophysics. 1994; 311:144–152. [PubMed: 8185311]

Sokoloff, L. The Joints and synovial fluid. Academic Press; New York: 1978.

Swann DA, Slayter HS, Silver FH. The Molecular-Structure of Lubricating Glycoprotein-I, the Boundary Lubricant for Articular-Cartilage. J Biol Chem. 1981; 256:5921–5925. [PubMed: 7240180]

Swanson, SAV. Friction, Wear, and Lubrication. In: Freeman, MAR., editor. Adult articular cartilage. 2d ed.. Pitman Medical, Tunbridge Wells, Eng.; 1979. p. 415-460.

Tam EM, Wu YI, Butler GS, Stack MS, Overall CM. Collagen binding properties of the membrane type-1 matrix metalloproteinase (MT1-MMP) hemopexin C domain - The ectodomain of the 44-kDa autocatalytic product of MT1-MMP inhibits cell invasion by disrupting native type I collagen cleavage. J Biol Chem. 2002; 277:39005–39014. [PubMed: 12145314]

Tocha E, Schonherr H, Vancso GJ. Quantitative nanotribology by AFM: A novel universal calibration platform. Langmuir. 2006; 22:2340–2350. [PubMed: 16489827]

Varenberg M, Etsion I, Halperin G. An improved wedge calibration method for lateral force in atomic force microscopy. Review of Scientific Instruments. 2003; 74:3362–3367.

Walters DA, Cleveland JP, Thomson NH, Hansma PK, Wendman MA, Gurley G, Elings V. Short cantilevers for atomic force microscopy. Review of Scientific Instruments. 1996; 67:3583–3590.

Zappone B, Ruths M, Greene GW, Jay GD, Israelachvili JN. Adsorption, lubrication, and wear of lubricin on model surfaces: Polymer brush-like behavior of a glycoprotein. Biophys J. 2007; 92:1693–1708. [PubMed: 17142292]

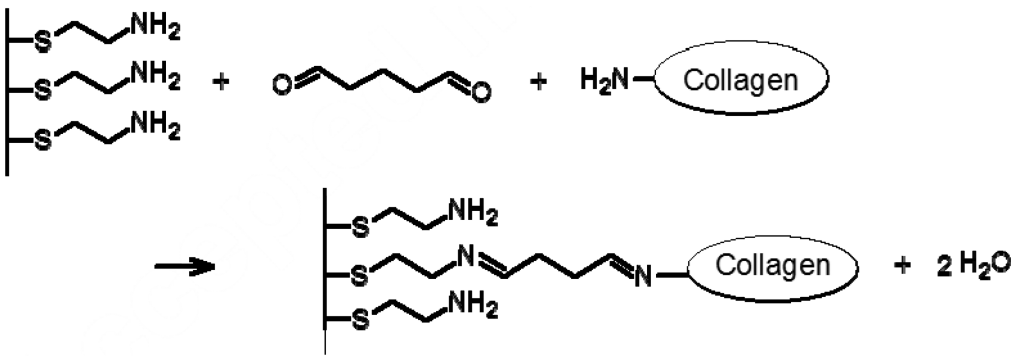

Figure 1.
Chemical attachment of collagen ton amine-functionalized surfaces with glutaraldehyde.

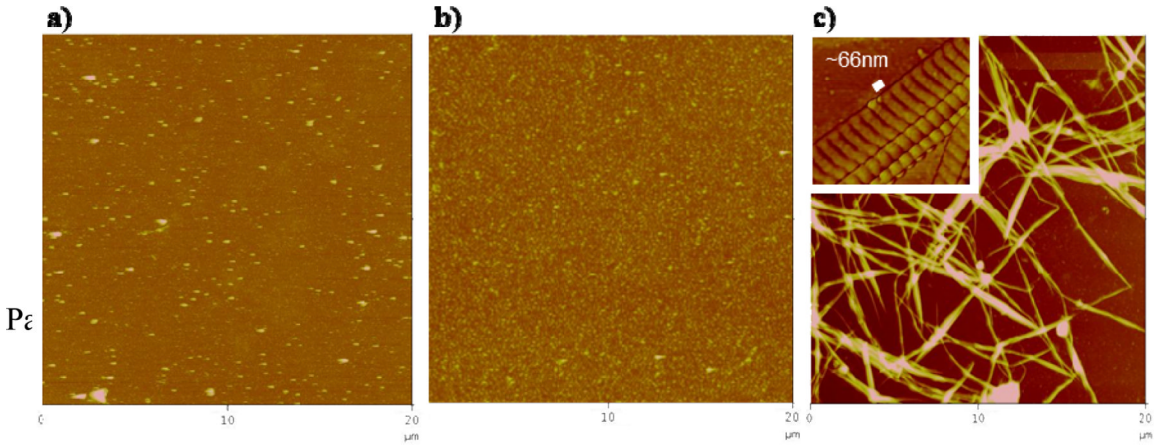

Figure 2.

Topographical AFM images of the a) denatured, b) amorphous and c) microfibrillar collagen surfaces (Z scale = 100, 100, and 200 nm, respectively). Inset: High magnification of the fibrillar collagen phase image, showing collagen molecules are staggered ~66 nm apart.

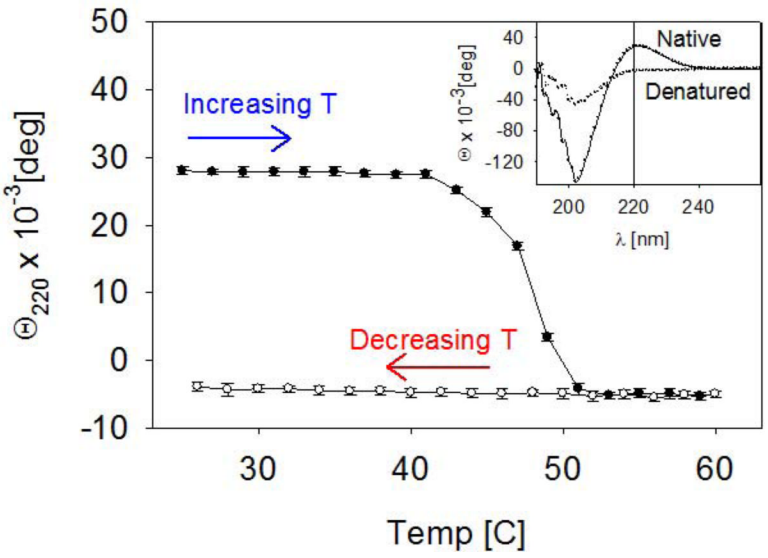

Figure 3.
Temperature dependence of the ellipticity of a collagen solution measured at 220 nm. The inset shows the circular dichroism spectra of native (helical) and denatured (random) collagen before and after heating.

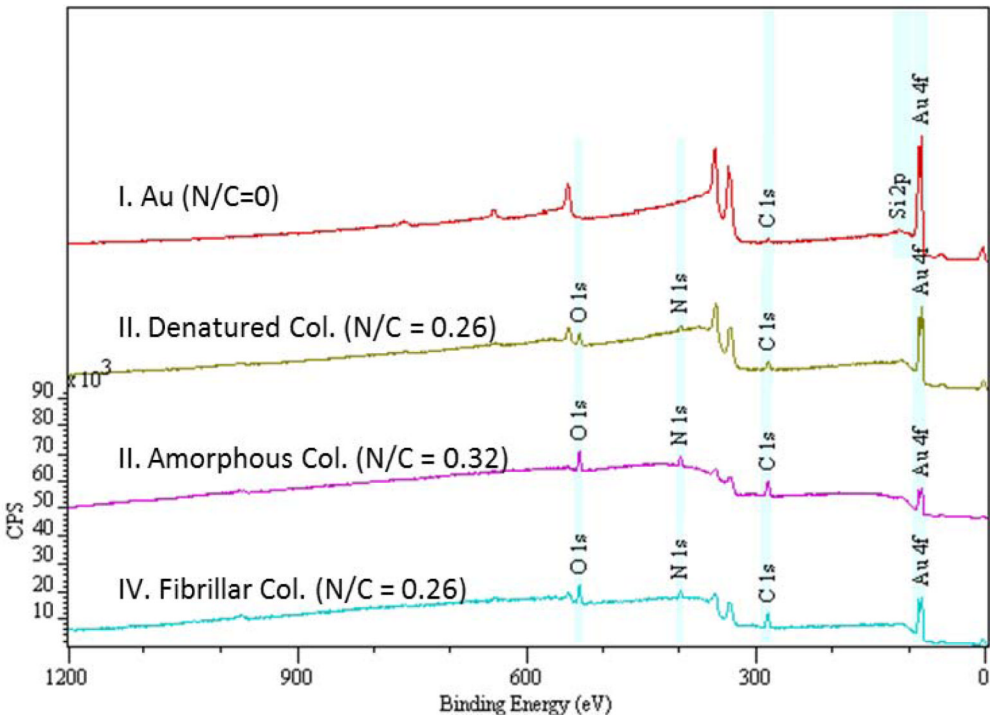

Figure 4.

XPS survey spectra of gold (I), denatured collagen (II), amorphous collagen (III) and fibrillar collagen (IV) surfaces along with their corresponding nitrogen to carbon (N/C) ratio. The spectra were offset in the Y direction for clarity.

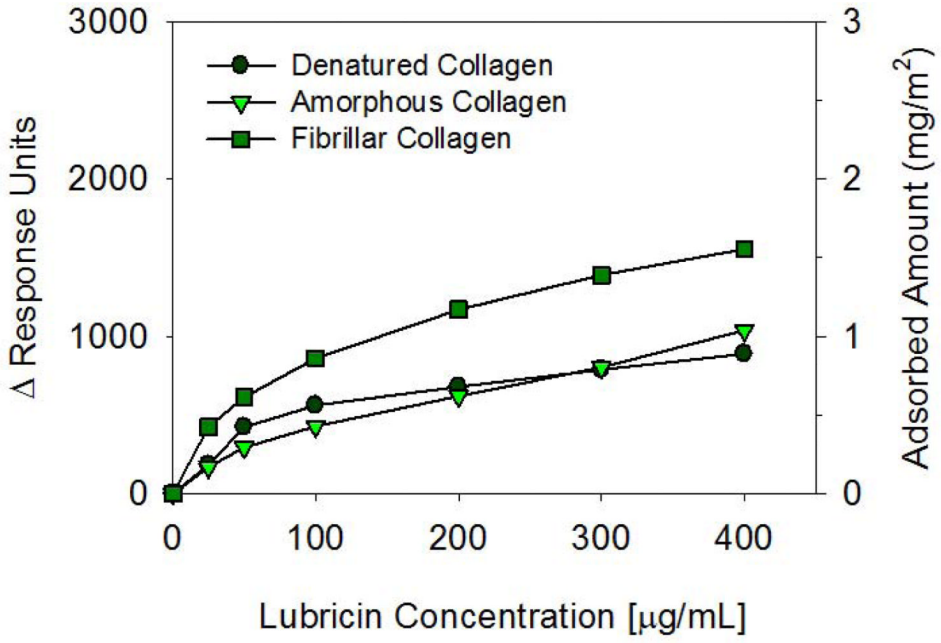

Figure 5.
Biacore SPR measurements of lubricin adsorption on denatured, amorphous, and fibrillar collagen surfaces as a function of concentration. A change in one response unit (ΔRU) corresponds to approximately 1pg/mm^2 of adsorbed globular protein.

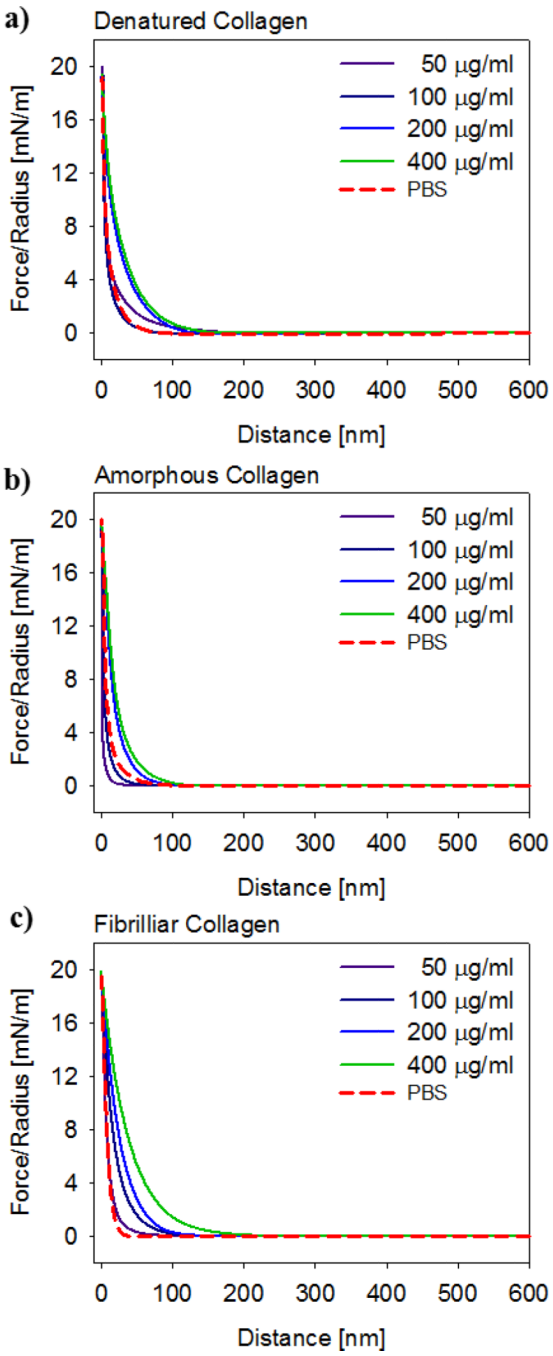

Figure 6.
Interaction force upon approach normalized by probe radius, plotted as a function of separation distance between a) denatured, b) amorphous, and c) fibrillar collagen surfaces, for a range of lubricin concentrations. Each curve represents an average of approximately 100 individual curves.

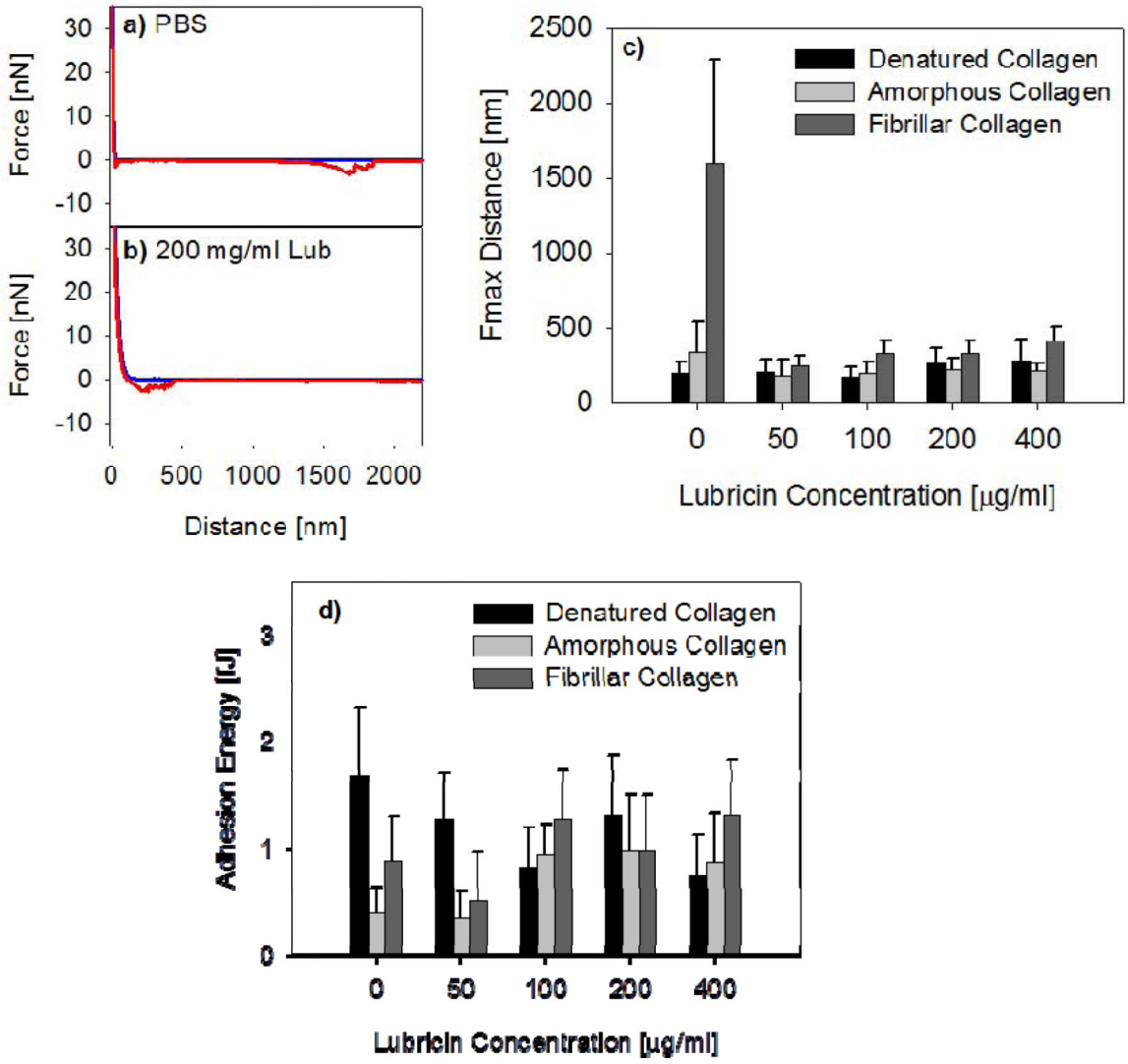

Figure 7.

Typical force curves between fibrillar collagen in a) PBS and in b) 200 μg/ml lubricin solution. c) Average distance at max pull-off force, F_{max} distance, and d) average adhesion energy, between three types of collagen surfaces, as a function of lubricin concentration. The error bars represent the standard deviation of the mean from measurements taken on 100 different locations.

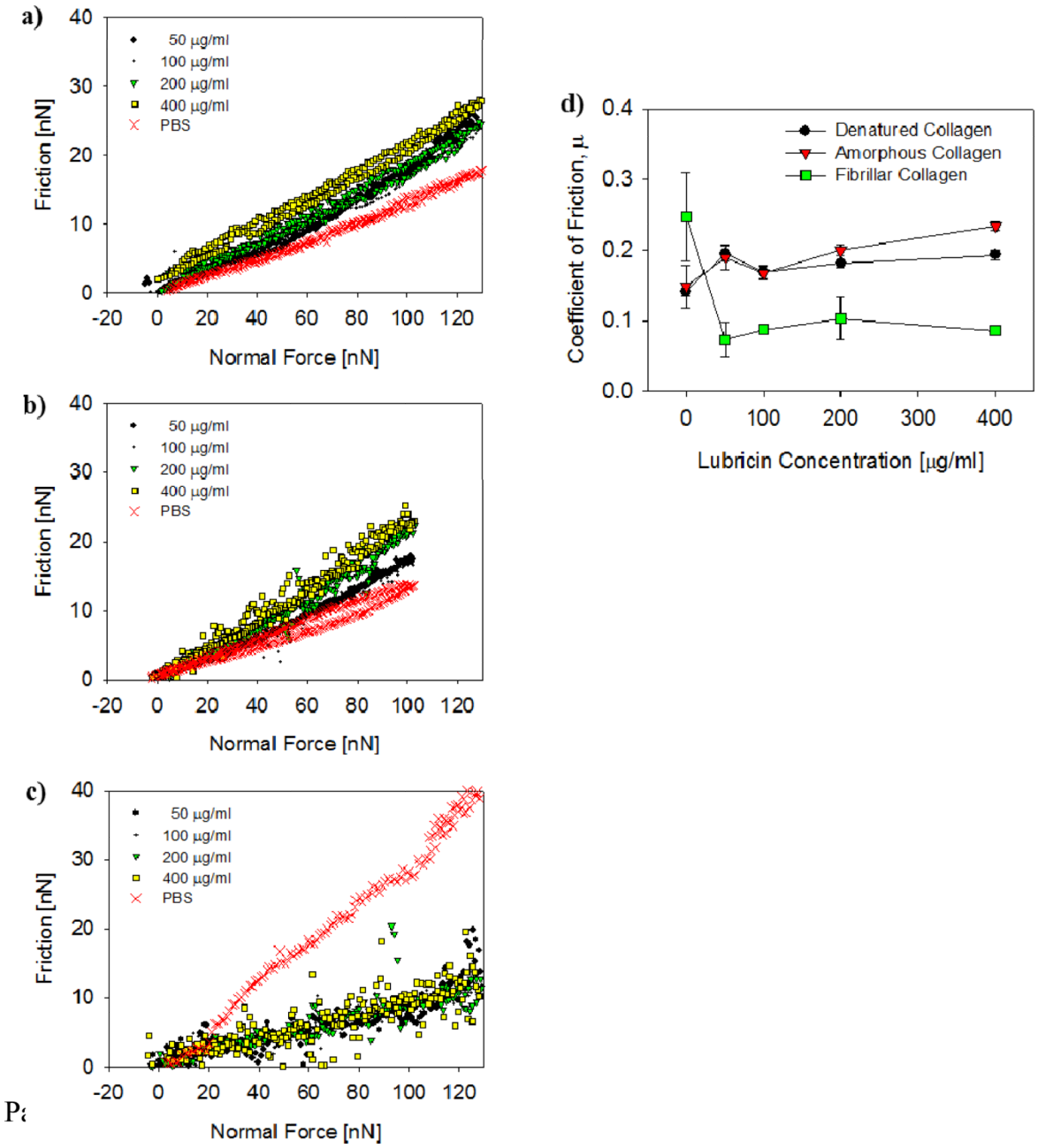

Figure 8.

Typical friction vs. normal force curves measured between a) denatured, b) amorphous, and c) fibrillar collagen surfaces, for a range of lubricin concentrations and in PBS. d) Coefficient of friction plotted vs. lubricin concentration for the tree different collagen surfaces shown in a-c). The error bars represent the standard deviation of the mean from friction measurements on 3 different locations.